*J. Plasma Phys.* (2016), *vol.* 82, 905820503  
doi:10.1017/S0022377816000830

# Sensitivity of kinetic ballooning mode instability to tokamak equilibrium implementations

**H. S. Xie[1,3], Y. Xiao[1,†], I. Holod[2], Z. Lin[2,3] and E. A. Belli[4]**

[1]Institute for Fusion Theory and Simulation, Department of Physics, Zhejiang University, Hangzhou 310027, PR China

[2]Department of Physics and Astronomy, University of California, Irvine, CA 92697, USA

[3]Fusion Simulation Center, Peking University, Beijing 100871, China

[4]General Atomics, P.O. Box 85608, San Diego, CA 92186-5608, USA

(Received 14 June 2016; revised 5 September 2016; accepted 7 September 2016)

Global, first-principles study of the kinetic ballooning mode (KBM) is crucial to understand tokamak edge physics in high-confinement mode (H-mode). In contrast to the ion temperature gradient mode and trapped electron mode, the KBM is found to be very sensitive to the equilibrium implementations in gyrokinetic codes. In this paper, we show that a second-order difference in Shafranov shift or geometric coordinates, or a difference between local and global profile implementations can bring a factor of two or more discrepancy in real frequency and growth rate. This suggests that an accurate global equilibrium is required for validation of gyrokinetic KBM simulations.

**Key words:** plasma confinement, plasma instabilities, plasma simulation

## 1. Introduction

The ballooning mode (Connor, Hastie & Taylor 1978) is an electromagnetic instability driven mainly by the pressure gradient, and is considered to be one of the most important instabilities in the high-confinement mode (H-mode) stage of tokamaks. The H-mode is important for tokamaks since it can improve the plasma confinement to make fusion more economically feasible. The ideal peeling-ballooning mode (Connor *et al.* 1998) and kinetic ballooning mode (KBM) (Tang, Connor & Hastie 1980; Belli & Candy 2010; Holod & Lin 2013; Tang *et al.* 2016) are invoked to predict the constraints of the H-mode pedestal (Snyder *et al.* 2011). The linear and nonlinear physics of the peeling-ballooning mode have recently been studied intensively with fluid codes, such as the eigenvalue code ELITE (Wilson *et al.* 2002) and initial value code BOUT++ (Dudson *et al.* 2009). These studies have helped explain several important aspects (e.g. mode numbers) of H-mode experiments (cf. Liu *et al.* 2014). However, the fluid model ignores many important kinetic effects, such as the wave–particle resonance and finite Larmor radius effect, which may play a critical role in the formation of the H-mode pedestal. A complete understanding of the electromagnetic instabilities in the tokamak edge is still in progress. Even

† Email address for correspondence: yxiao@zju.edu.cn

after one decade of efforts, gyrokinetic electromagnetic simulation is still working on code–code verification due to its great challenge.

As an effort of code verification, the linear properties of the KBM have recently been compared amongst various gyrokinetic continuum codes, including GS2 (Bourdelle *et al.* 2003; Joiner, Hirose & Dorland 2010) and GYRO (Belli & Candy 2010; Moradi *et al.* 2012). The KBM is found to be sensitive to parallel magnetic fluctuation (Belli & Candy 2010) and the treatment of the radial pressure gradient term in the drift velocity (Belli & Candy 2010). The parallel magnetic fluctuation is not considered in this paper. Regarding the radial pressure gradient term, this effect may be particular to flux-tube continuum codes, as the pressure gradient-driven magnetic drift is automatically included in gyrokinetic particle simulations (Holod *et al.* 2009). A newly published paper (Gorler *et al.* 2016) using the continuum code GENE shows that in order to obtain consistent linear growth rates, a radially global simulation model must be used. However, the details of the global equilibrium profile model used in this study were not specified. In this paper, we use gyrokinetic particle simulations to emphasize that, even in global simulations, the details of the equilibrium magnetic configuration are important for studies of the KBM. In contrast, they are not critical for electrostatic simulation, such as for the standard ion temperature gradient (ITG) mode or trapped electron mode (TEM). The stabilization effect of the Shafranov shift on the KBM is also demonstrated by our simulations. This suggests that, for the purpose of experimental validation, the realistic Shafranov shift is an indispensable component (Moradi *et al.* 2014; Citrin *et al.* 2015). In addition, the global radial profile of the plasma equilibrium is important for electromagnetic simulations such as for the KBM, while for electrostatic ITG/TEM simulation, the linear growth rate and frequency depend only on the peak value of the global gradients.

For electrostatic simulations of tokamak plasmas, the equilibrium magnetic geometry is critical for quantitative study of the nonlinear physics (Xiao & Catto 2006; Lapillonne *et al.* 2009; Lin *et al.* 2012). GTC has recently implemented real tokamak geometry (Xiao *et al.* 2015) from EFIT (Lao *et al.* 1985)/VMEC (Hirshman & Whitson 1983) for experimental validations (cf. Wang *et al.* 2013). It has been found that ignoring the difference in the poloidal angle between torus coordinates $(r, \theta_0, \zeta_0)$ and flux coordinates $(r_f, \theta_f, \zeta_f)$ could lead to significant differences in the turbulent transport simulated by various gyrokinetic codes (Lin & Hahm 2004; Lapillonne *et al.* 2009; Lin *et al.* 2012). For electromagnetic simulations of finite-$\beta$ plasmas, the electromagnetic effect may dominate. The electromagnetic capability has been implemented in the global gyrokinetic simulation code GTC (Holod *et al.* 2009). The semi-analytical, global Shafranov equilibrium is implemented (Xie 2014; Xie 2015; Xiao *et al.* 2015) to second order in the GTC code to study the magnetic equilibrium effects for the electromagnetic KBM. It is found that a slight difference in the equilibrium can cause a large difference in the linear KBM frequency and growth rate. The local and global profiles also provide rather different linear frequencies and growth rates.

## 2. Equilibrium sensitivity

In this work, we consider a low-$\beta$ model equilibrium with $\beta \sim \epsilon^2$, where $\epsilon = r/R_0 \ll 1$ is the inverse aspect ratio. Under the boundary condition given by a circular conducting wall, the equilibrium flux surfaces are concentric circles to lowest order. To second order, the flux surfaces are shifted circles, which can be

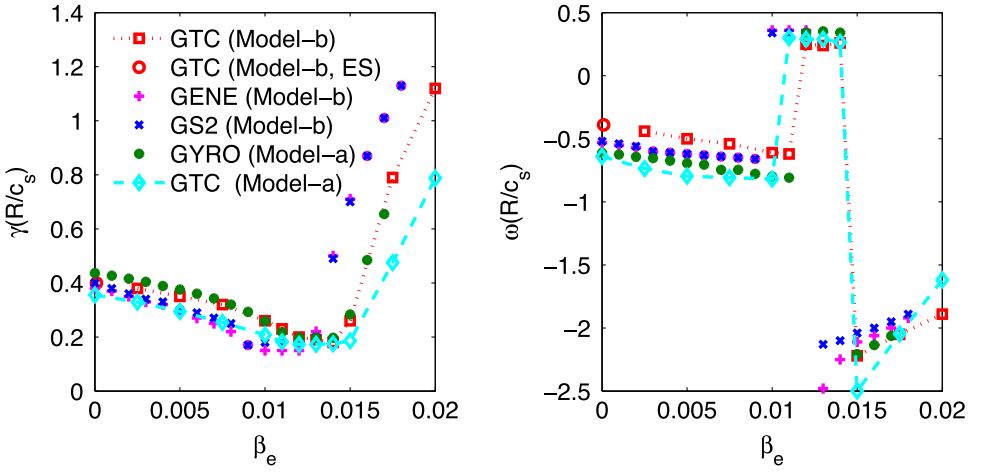


FIGURE 1. Scan over $\beta_e$ comparing GTC with other gyrokinetic codes (GYRO, GENE and GS2) for different equilibrium field models. The transition from ITG to TEM and to KBM is clearly shown as $\beta_e$ increases. The equilibrium implementations do not affect the ITG and TEM significantly, but do affect the KBM branch significantly. Data are partly taken from Candy (2005), Pueschel, Kammerer & Jenko (2008), Belli & Candy (2010), Holod & Lin (2013). ES means electrostatic simulation.

defined in terms of the usual cylindrical coordinates $(R, \phi_c, Z)$ by the following equations:

$$R = R_0 + r_s \cos\theta_s - \Delta(r_s), \tag{2.1a}$$

$$\phi_c = -\zeta_s, \tag{2.1b}$$

$$Z = r_s \sin\theta_s, \tag{2.1c}$$

where $R_0$ is the major radius and the Shafranov shift $\Delta(0) = 0$. (Note: some authors use $\Delta|_{r_s=a} = 0$, where $a$ is the minor radius. However, what really matters is the derivative of the Shafranov shift.) The relations between Boozer flux coordinates $(r_f, \theta_f, \zeta_f)$ and geometry coordinates $(r_s, \theta_s, \zeta_s)$ are $r = r_s$, $\zeta_f = \zeta_s$ and $\theta_f = \theta_s - (\epsilon + \Delta')\sin\theta_s$ (Meiss & Hazeltine 1990). Here $\Delta'$ is the radial derivative of the Shafranov shift $\Delta(r) = \int_0^r ((q^2\,\mathrm{d}r)/(r^3 R_0)) \int_0^r [r^2/q^2 - 2(R_0^2/B_0^2)rp']r\,\mathrm{d}r$ (White 2001), where $q$ is the safety factor, $B_0$ is the on-axis magnetic field and $p$ is the normalized pressure. In the gyrokinetic community, three types of so called $s$–$\alpha$ models ($s = (r/q)\,\mathrm{d}q/\mathrm{d}r$, $\alpha = -R_0 q^2 \beta'$, where $\beta$ is the ratio between plasma and magnetic field pressures) are generally used, with Model-a: lowest-order approximation $\theta = \theta_s$, Model-b: first-order approximation without the Shafranov shift, $\Delta = 0$ and $\theta = \theta_s - \epsilon \sin\theta_s$ and Model-c: $\Delta \neq 0$ and $\theta = \theta_s - (\epsilon + \Delta')\sin\theta_s$. Model-a and Model-b differ in the definition of poloidal angle $\theta$. In Model-a, the poloidal angle $\theta$ is simplified as the geometric poloidal angle. In Model-b, the poloidal angle is a flux coordinate and contains higher-order corrections in $\epsilon$.

Figure 1 shows the linear frequency and growth rate for a scan over $\beta_e$, comparing the GTC results with those from other gyrokinetic codes (GYRO, GENE and GS2). Here the Cyclone base case parameters (Dimits *et al.* 2000) are employed, i.e. $s = 0.78$, $q = 1.4$, $r/R_0 = 0.18$, $R_0/L_T = 6.9$, $R_0/L_n = 2.2$ and $T_i = T_e$, where $L_n = -\mathrm{d}\ln n/\mathrm{d}r$ and $L_T = -\mathrm{d}\ln T/\mathrm{d}r$. Also, $k_\theta \rho_i = 0.22$, where $k_\theta = nq/r$ and $\rho_i = \sqrt{T_i/m_i}/\Omega_{ci}$

is the ion Larmor radius. In addition, the following parameters are used in the simulation: $m_i/m_e = 1837$, $R_0 = 83.5$ cm, $\rho_i/a = 125$, $B_0 = 2.0T$, $T_e = T_i = 2.2$ keV. We set-up different $\beta_e$ parameters by varying the electron density $n_e$ (Holod & Lin 2013), e.g. for $\beta_e = 2.0\,\%$, $n_e = 0.90 \times 10^{14}$ cm$^{-3}$. In figure 1, the data for GENE/GS2/GYRO are interpolated from the original data with $k_\theta \rho_i = 0.20$ and 0.25 in Candy (2005), Pueschel *et al.* (2008), Belli & Candy (2010). The transition from ITG (ion temperature gradient mode) to TEM (trapped electron mode) and to KBM is clearly shown as $\beta_e$ increases. The GTC (Model-b) electromagnetic (Holod *et al.* 2009; Holod & Lin 2013) simulation recovers the GTC (Model-b, ES) electrostatic (Lin & Hahm 2004) result as $\beta_e \to 0$. This shows that the GTC electromagnetic simulation converges to the electrostatic simulation in the low-$\beta$ limit. In figure 1 the equilibrium implemented in GYRO is Model-a while that in GS2/GENE is Model-b by default. In the GTC code, both Model-a and Model-b are implemented. As can been seen in figure 1, while the equilibrium implementation does not largely affect the ITG, TEM and their transitions, it does significantly affect the linear growth rate of KBM. The GTC code gives a real frequency for the KBM branch similar to the other gyrokinetic codes, but gives a smaller growth rate. For example, for the case with $\beta_e = 1.75\,\%$ and Model-a, $\gamma^{GYRO} \simeq 1.5\gamma^{GTC}$. We note that this difference could come from the difference in the equilibrium profiles, as is shown in the latter part of this paper. That is, other gyrokinetic codes like GYRO use local flux-tube geometry, whereas the GTC code uses a global geometry. A linear electromagnetic gyrokinetic study has previously been carried out for the DIII-D H-mode pedestal (Wang *et al.* 2012), which shows that the frequency and growth rate can have a 50 % deviation among several gyrokinetic codes with local equilibrium settings. We also note that the gyrokinetic code GEM with flux-tube equilibrium shows good agreement with the aforementioned gyrokinetic codes such as GYRO for the ITG and TEM instabilities based on a different set of parameters (Chen *et al.* 2013).

To further quantify the effect of the equilibrium implementation, figure 2 shows a more detailed scan of $\beta_e$ (with $k_\theta \rho_i = 0.22$) and $k_\theta \rho_i$ (with $\beta_e = 1.75\,\%$) for the KBM branch. It is well known that Shafranov shift has a great effect on the stability of the KBM (Moradi *et al.* 2014; Citrin *et al.* 2015). Indeed, we find a large discrepancy in both the frequency and growth rate if the Shafranov shift is considered in the GTC simulation, as shown in figure 2. Both $\omega$ and $\gamma$ become much smaller in magnitude when the Shafranov shift is included. It is observed that the electromagnetic perturbations still dominate the electrostatic perturbations, with $A_\parallel/\phi \sim 3$–$6$ in ideal Alfvén wave units (i.e. $A_\parallel/\phi = 1$ for the ideal Alfvén eigenmode). This suggests that the mode is still an electromagnetic mode, such as a KBM. In addition, we have also compared the Shafranov shift effect on the ITG instability. In the GTC simulation, the differences in $\omega$ and $\gamma$ between equilibriums with and without Shafranov shift are less than 5 % (Xie 2014; Xie 2015).

These findings suggest that an accurate global equilibrium, rather than a local equilibrium model, is crucial to validate experiments with gyrokinetic simulations. Another important factor for the gyrokinetic simulation is the density and temperature profiles and their associated gradients. To illustrate that the local profiles may not be suitable for validating experiments described by the KBM, we compare results from various equilibrium profiles using the GTC code. In figures 1 and 2, the following global profile ('default test') for GTC is used: $q = 0.82 + 1.1(\psi/\psi_w) + 1.0(\psi/\psi_w)^2$, $n_i = n_e = 1.0 + 0.205\{\tanh[(0.3 - (\psi/\psi_w))/0.4] - 1.0\}$ and $T_i = T_e = 1.0 + 0.415\{\tanh[(0.18 - (\psi/\psi_w))/0.4] - 1.0\}$. Here $\psi$ is the poloidal flux and $\psi_w = \psi(r = a) = 0.0375 B_0 R_0^2$, which gives $a/R_0 = 0.36$. The local parameters at

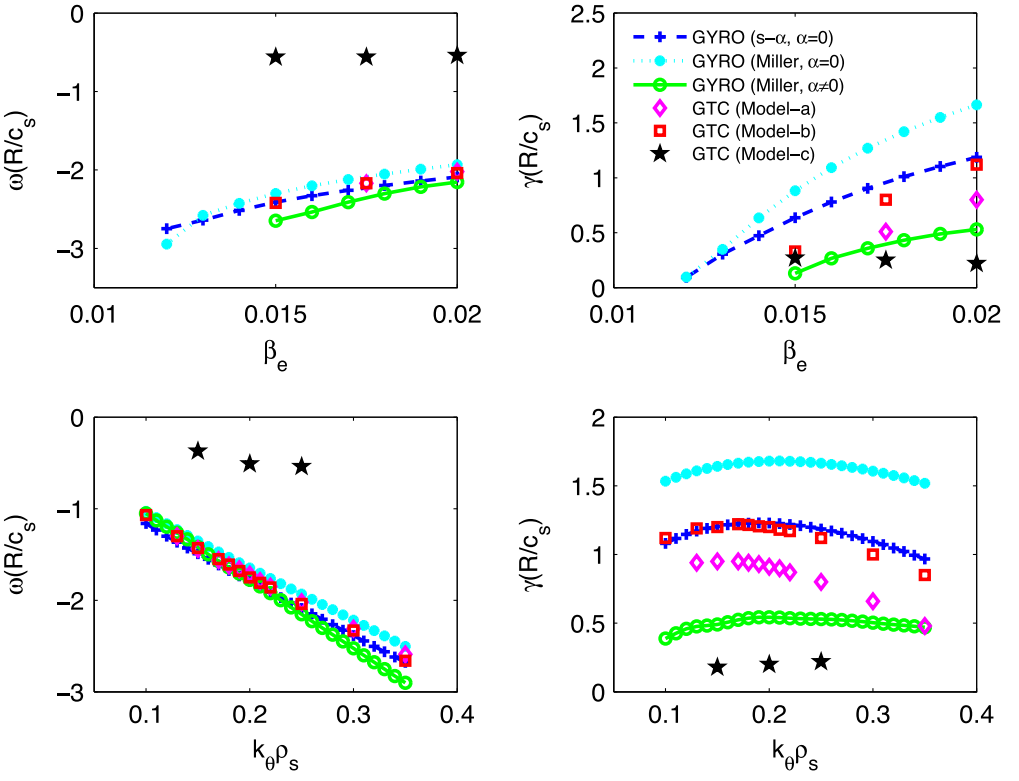


FIGURE 2. GTC versus GYRO for different equilibrium implementations. GYRO ($s$–$\alpha$, $\alpha = 0$) is Model-a; GYRO (Miller, $\alpha = 0$) is Model-b; GYRO (Miller, $\alpha \neq 0$) is Model-c.

$r = 0.5a$ (which is the position where the density and temperature profiles peak) are the same as the Cyclone base case. To model the local equilibrium profile, we use the following gradients to calculate the density and temperature profiles: $R_0/L_n = 2.22\mathrm{e}^{-[(r/a-0.5)/\Delta r]^6}$ and $R_0/L_T = 6.92\mathrm{e}^{-[(r/a-0.5)/\Delta r]^6}$, where $\Delta r$ is the radial width of the local profile. The density and temperature profiles are reproduced to be consistent with these gradient profiles. Figure 3 shows the $R_0/L_n$ used in GTC to model local equilibrium profiles, where the plateau gradient equals the peak value of the test gradient profile. In the electrostatic simulations for the ITG and TEM, the linear frequency and growth rate are not sensitive to $\Delta r$. Table 1 shows the electromagnetic simulation results for the ITG and KBM with different local profile widths $\Delta r$. We see that the frequency and growth rate for ITG change little for different equilibrium profile implementations. However, the frequency and growth rate for the KBM change by approximately 25 % for different equilibrium profile implementations. To ensure that this difference comes from the equilibrium, in the above simulations, the massless fluid model for electrons (Lin & Chen 2001; Holod *et al.* 2009) (where the TEM is excluded) and Model-a equilibrium (to exclude the Shafranov shift) are used. The only difference between the ITG and KBM simulations is $\beta_e$, i.e. $\beta_e^{ITG} = 0.25\,\%$ and $\beta_e^{KBM} = 1.75\,\%$ respectively. The results confirm that the KBM is very sensitive to the equilibrium profiles. This sensitivity to the radial profile may be caused by the relatively larger radial extension of the KBM. To fully understand this issue, further analytic investigation is required. Overall, this suggests

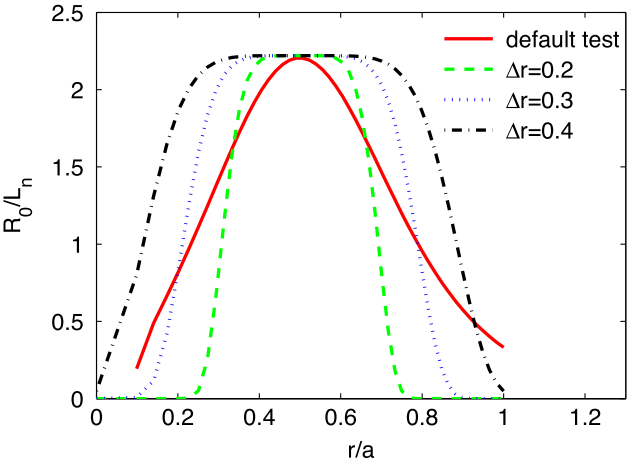


FIGURE 3. Various equilibrium profiles of $R_0/L_n$ used in GTC.

| $\omega$ | $\Delta r = 0.4$ | $\Delta r = 0.3$ | $\Delta r = 0.2$ | Default test |
|---|---|---|---|---|
| KBM | $1.67 + 1.09i$ | $1.77 + 1.02i$ | $1.90 + 0.93i$ | $2.06 + 0.75i$ |
| ITG | $0.47 + 0.16i$ | $0.47 + 0.15i$ | $0.48 + 0.14i$ | $0.50 + 0.13i$ |

TABLE 1. Influence of the radial width of the local profiles on the KBM and ITG. Here, in contrast to figures 1 and 2, a massless fluid model for electrons is used.

that an exact global equilibrium, such as from EFIT/VMEC, needs to be used in gyrokinetic simulations to verify codes and to validate experiments with the KBM as the dominant instability.

## 3. Summary and discussion

We report that the linear physics of the KBM, in contrast to the ITG and TEM, is extremely sensitive to the equilibrium implementation in the gyrokinetic code. A second-order difference in the magnetic equilibrium can result in a factor of two or more difference in the real frequency and growth rate. This suggests that an accurate global equilibrium is required for validation of gyrokinetic simulations of the KBM.

## Acknowledgements

H.S.X. would like to thank X. Q. Xu for useful discussions and J. Candy for information on the $s$–$\alpha$ model. The work is supported by the National Magnetic Confinement Fusion Energy Program under grant nos. 2015GB110000, 2013GB111000, China NSFC under grant no. 11575158, the Recruitment Program of Global Youth Experts, and US DOE SciDac GSEP centers.

## REFERENCES

BELLI, E. A. & CANDY, J. 2010 Fully electromagnetic gyrokinetic eigenmode analysis of high-beta shaped plasmas. *Phys. Plasmas* **17** (11), 112314.

BOURDELLE, C., DORLAND, W., GARBET, X., HAMMETT, G. W., KOTSCHENREUTHER, M., REWOLDT, G. & SYNAKOWSKI, E. J. 2003 Stabilizing impact of high gradient of beta on microturbulence. *Phys. Plasmas* **10** (7), 2881–2887.

CANDY, J. 2005 Beta scaling of transport in microturbulence simulations. *Phys. Plasmas* **12** (7), 072307.

CHEN, Y., PARKER, S. E., WAN, W. & BRAVENEC, R. 2013 Benchmarking gyrokinetic simulations in a toroidal flux-tube. *Phys. Plasmas* **20** (9), 092511.

CITRIN, J., GARCIA, J., GORLER, T., JENKO, F., MANTICA, P., TOLD, D., BOURDELLE, C., HATCH, D. R., HOGEWEIJ, G. M. D., JOHNSON, T. *et al.* 2015 Electromagnetic stabilization of tokamak microturbulence in a high-beta regime. *Plasma Phys. Control. Fusion* **57** (1), 014032.

CONNOR, J. W., HASTIE, R. J. & TAYLOR, J. B. 1978 Shear, periodicity, and plasma ballooning modes. *Phys. Rev. Lett.* **40** (6), 396–399.

CONNOR, J. W., HASTIE, R. J., WILSON, H. R. & MILLER, R. L. 1998 Magnetohydrodynamic stability of tokamak edge plasmas. *Phys. Plasmas* **5** (7), 2687–2700.

DIMITS, A. M., BATEMAN, G., BEER, M. A., COHEN, B. I., DORLAND, W., HAMMETT, G. W., KIM, C., KINSEY, J. E., KOTSCHENREUTHER, M., KRITZ, A. H. *et al.* 2000 Comparisons and physics basis of tokamak transport models and turbulence simulations. *Phys. Plasmas* **7**, 969.

DUDSON, B. D., UMANSKY, M. V., XU, X. Q., SNYDER, P. B. & WILSON, H. R. 2009 Bout++: a framework for parallel plasma fluid simulations. *Comput. Phys. Commun.* **180** (9), 1467–1480.

GORLER, T., TRONKO, N., HORNSBY, W. A., BOTTINO, A., KLEIBER, R., NORSCINI, C., GRANDGIRARD, V., JENKO, F. & SONNENDRUCKER, E. 2016 Intercode comparison of gyrokinetic global electromagnetic modes. *Phys. Plasmas* **23** (7), 072503.

HIRSHMAN, S. P. & WHITSON, J. C. 1983 Steepest descent moment method for three dimensional magnetohydrodynamic equilibria. *Phys. Fluids* **26** (12), 3553–3568.

HOLOD, I. & LIN, Z. 2013 Verification of electromagnetic fluid–kinetic hybrid electron model in global gyrokinetic particle simulation. *Phys. Plasmas* **20** (3), 032309.

HOLOD, I., ZHANG, W. L., XIAO, Y. & LIN, Z. 2009 Electromagnetic formulation of global gyrokinetic particle simulation in toroidal geometry. *Phys. Plasmas* **16** (12), 122307.

JOINER, N., HIROSE, A. & DORLAND, W. 2010 Parallel magnetic field perturbations in gyrokinetic simulations. *Phys. Plasmas* **17** (7), 072104.

LAO, L. L., GREENE, J. M., WANG, T. S., HELTON, F. J. & ZAWADZKI, E. M. 1985 Three-dimensional toroidal equilibria and stability by a variational spectral method. *Phys. Fluids* **28** (3), 869–877.

LAPILLONNE, X., BRUNNER, S., DANNERT, T., JOLLIET, S., MARINONI, A., VILLARD, L., GORLER, T., JENKO, F. & MERZ, F. 2009 Clarifications to the limitations of the s-alpha equilibrium model for gyrokinetic computations of turbulence. *Phys. Plasmas* **16** (3), 032308.

LIN, Z. & CHEN, L. 2001 A fluid–kinetic hybrid electron model for electromagnetic simulations. *Phys. Plasmas* **8** (5), 1447–1450.

LIN, Z., ETHIER, S., HAHM, T. S. & TANG, W. M. 2012 Verification of gyrokinetic particle simulation of device size scaling of turbulent transport. *Plasma Sci. Technol.* **14** (12), 1125.

LIN, Z. & HAHM, T. S. 2004 Turbulence spreading and transport scaling in global gyrokinetic particle simulations. *Phys. Plasmas* **11** (3), 1099–1108.

LIU, Z. X., XU, X. Q., GAO, X., XIA, T. Y., JOSEPH, I., MEYER, W. H., LIU, S. C., XU, G. S., SHAO, L. M. & DING, S. Y. 2014 Three dimensional nonlinear simulations of edge localized modes on the east tokamak using bout++ code. *Phys. Plasmas* **21** (9), 090705.

MEISS, J. D. & HAZELTINE, R. D. 1990 Canonical coordinates for guiding center particles. *Phys. Fluids* B **2** (11), 2563–2567.

MORADI, S., PUSZTAI, I., MOLLEN, A. & FULOP, T. 2012 Impurity transport due to electromagnetic drift wave turbulence. *Phys. Plasmas* **19** (3), 032301.

MORADI, S., PUSZTAI, I., VOITSEKHOVITCH, I., GARZOTTI, L., BOURDELLE, C., PUESCHEL, M. J., LUPELLI, I., ROMANELLI, M. & THE JET-EFDA CONTRIBUTORS 2014 Core micro-instability analysis of jet hybrid and baseline discharges with carbon wall. *Nucl. Fusion* **54** (12), 123016.

PUESCHEL, M. J., KAMMERER, M. & JENKO, F. 2008 Gyrokinetic turbulence simulations at high plasma beta. *Phys. Plasmas* **15** (10), 102310.

SNYDER, P. B., GROEBNER, R. J., HUGHES, J. W., OSBORNE, T. H., BEURSKENS, M., LEONARD, A. W., WILSON, H. R. & XU, X. Q. 2011 A first-principles predictive model of the pedestal

height and width: development, testing and iter optimization with the eped model. *Nucl. Fusion* **51** (10), 103016.

TANG, W. M., CONNOR, J. W. & HASTIE, R. J. 1980 Kinetic-ballooning-mode theory in general geometry. *Nucl. Fusion* **20** (11), 1439.

TANG, T. F., XU, X. Q., MA, C. H., BASS, E. M., HOLLAND, C. & CANDY, J. 2016 Benchmark studies of the gyro-landau-fluid code and gyro-kinetic codes on kinetic ballooning modes. *Phys. Plasmas* **23** (3), 032119.

WANG, Z., LIN, Z., HOLOD, I., HEIDBRINK, W. W., TOBIAS, B., VAN ZEELAND, M. & AUSTIN, M. E. 2013 Radial localization of toroidicity-induced alfvén eigenmodes. *Phys. Rev. Lett.* **111**, 145003.

WANG, E., XU, X., CANDY, J., GROEBNER, R. J., SNYDER, P. B., CHEN, Y., PARKER, S. E., WAN, W., LU, G. & DONG, J. Q. 2012 Linear gyrokinetic analysis of a diii-d h-mode pedestal near the ideal ballooning threshold. *Nucl. Fusion* **52** (10), 103015.

WHITE, R. B. 2001 *The Theory of Toroidally Confined Plasmas*. World Scientific Imperial College Press,; (revised second edition 2006).

WILSON, H. R., SNYDER, P. B., HUYSMANS, G. T. A. & MILLER, R. L. 2002 Numerical studies of edge localized instabilities in tokamaks. *Phys. Plasmas* **9** (4), 1277–1286.

XIAO, Y. & CATTO, P. J. 2006 Plasma shaping effects on the collisionless residual zonal flow level. *Phys. Plasmas* **13**, 082307.

XIAO, Y., HOLOD, I., WANG, Z., LIN, Z. & ZHANG, T. 2015 Gyrokinetic particle simulation of microturbulence for general magnetic geometry and experimental profiles. *Phys. Plasmas* **22** (2), 022516.

XIE, H.-S. 2014 Shifted circular tokamak equilibrium with application examples (unpublished notes http://hsxie.me/codes/shafeq/).

XIE, H.-S. 2015 Numerical simulations of micro-turbulence in tokamak edge. PhD thesis, Zhejiang University.